Proceedings of the 28th IEEE
EMBS Annual International Conference
New York City, USA, Aug 30-Sept 3, 2006

Multiday Electrophysiological Recordings from Freely Behaving Primates

Vikash Gilja[‡], Michael D. Linderman[*], Gopal Santhanam[*], Afsheen Afshar[*§],
Stephen Ryu[*¶], Teresa H. Meng[*], Krishna V. Shenoy[*†]
[*]Department of Electrical Engineering [‡]Department of Computer Science
[§]School of Medicine [¶]Department of Neurosurgery [†]Neurosciences Program
Stanford University, Stanford, California, USA

Abstract— **Continuous multiday broadband neural data provide a means for observing effects at fine timescales over long periods. In this paper we present analyses on such data sets to demonstrate neural correlates for physically active and inactive time periods, as defined by the response of a head-mounted accelerometer. During active periods, we found that 5–25 Hz local field potential (LFP) power was significantly reduced, firing rate variability increased, and firing rates have greater temporal correlation. Using a single threshold fit to LFP power, 93% of the 403 5 minute blocks tested were correctly classified as active or inactive (as labeled by thresholding each block's maximal accelerometer magnitude). These initial results motivate the use of such data sets for testing neural prosthetics systems and for finding the neural correlates of natural behaviors.**

I. Introduction

Current experimental protocols limit awake and behaving primate electrophysiological studies to timescales of a few hours. Tracking neural signals over days involves patching together data sets separated by many hours, leaving large periods over which signals are unobserved. In order to comply with the limitations of recording equipment, behavior is generally constrained by chairing and head posting.

Recent advances in neural recording systems [2], [3] have enabled recording during primate free behavior. However, these systems can not produce multiday broadband neural data sets. In order to analyze the neural correlates of behavior over long time periods, spike sorts must be accurate. Broadband data sets are necessary to produce reliable spike sorts, as spike waveform shape can vary over time [4]. The HermesB system, introduced in [1], provides this capability.

These data sets can aid in the development of practical neural prosthetics systems. In order to maximize the benefit of such systems, prosthetics must be sensitive to neural changes across the day and must react robustly in the face of variable background conditions. For example, such systems should reliably detect whether the user is awake or asleep. If a neural prosthetic attempts to decode the users intentions during sleep, it may waste battery power or cause undesired behaviors. If such a system does not reliably detect waking periods, the user may lose the ability to interact with the world.

Thus, in this paper we present preliminary multiday broadband neural data recorded from a freely behaving macaque monkey. Specific attention is paid towards understanding systematic differences in firing rate and local field potential (LFP) during active and inactive periods.

This work was supported in part by MARCO Center for Circuit & System Solutions (T.H.M.,M.D.L.), NDSEG (V.G.,M.D.L.,G.S.) and NSF (V.G.,G.S.) fellowships, Bio-X Fellowship (A.A.), Christopher Reeve Paralysis Foundation (S.I.R.,K.V.S) and the following awards to K.V.S.: NSF Center for Neuromorphic Systems Engineering at Caltech, ONR Adaptive Neural Systems, Whitaker Foundation, Center for Integrated Systems at Stanford, Sloan Foundation, and Burroughs Wellcome Fund Career Award in the Biomedical Sciences. Please address correspondence to gilja@stanford.edu.

II. Methods

Using the HermesB system [1], single and multi-unit signals were recorded from a 96 channel electrode array (Cyberkinetics Neurotechnology Systems Inc.) chronically implanted in the dorsal premotor cortex (PMd) of an adult macaque monkey (August 2005). Surgical methods are described in [5], [6]. All experiments and procedures were approved by the Stanford University Institutional Animal Care and Use Committee (IACUC). The HermesB system is a portable neural recording system in a shielded chassis on the monkey's head, allowing free behavior in the home cage [1]. Data were recorded at a 67% duty cycle (5 minutes of recording, followed by 2.5 minutes of system sleep). Two neural channels were recorded per data set in full broadband (0.5–7.5 kHz with 12 bits of precision at 30 kSamples/s) and a head-mounted 3-axis accelerometer was recorded with 12 bits of precision at 1 kSamples/s. With these recording parameters, the battery life of the HermesB system is approximately 18 hours. A 54 hour data set was assembled by head posting the monkey and swapping the batteries every 18 hours. These pit stops required approximately 45 minutes of interaction with the monkey, with under 20 minutes of head posting. The lights were on in the housing room from approximately 07:00 to 19:00 and were off for the remainder of the day.

The recorded neural signals from each 5 minute block were post-processed with the Sahani spike sorting algorithm [7], [8]. Spike times were identified using a threshold determined from data across the block (3σ with respect to the RMS noise estimate from filtered data). A spike waveform, or snippet comprised of a 32 sample window around the threshold event, was extracted and aligned to its center of mass (COM). Snippets were projected into a 4-dimensional robust, noise-whitened principle components space (NWrPCA) and clustered using a maximum *a posteriori* (MAP) clustering tech-

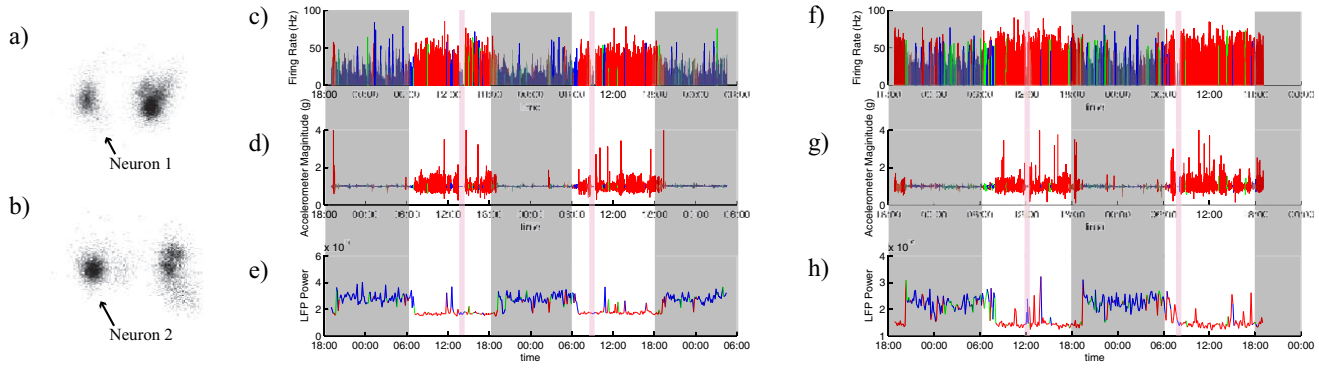

Fig. 1. Neural and accelerometer data recorded from a freely behaving monkey. (a,b) Histogram of spike waveform projections into NWrPCA space from two different electrodes recorded for different 54 hour data sets, selected neurons are indicated by arrows. (c) Firing rate of neuron 1 recorded over 54 hours. (d) Accelerometer magnitude over the recording period. (e) 5–25 Hz LFP power recorded from the same electrode. (f–h) Same plots for neuron 2. In all plots red and blue data points were recorded in time periods labeled as "active" and "inactive," respectively. Green data points were recorded during unlabeled periods. The wide light gray regions indicate night, and the thin pink regions indicate "pit stops," when the monkey was taken from the home cage and placed in a primate chair to service the recording equipment. (`D20060302.ch2u1 & D20060225.ch1u1`)

nique. Well-isolated units were identified and cross-referenced across blocks by hand.

LFPs were isolated from broadband data by applying Chebyshev Type I lowpass and bandpass filters with a passband ripple of 1 dB. Power spectral density estimates were calculated using the Welch periodgram method.

III. Results

Each five minute data block was either labeled as "active" or "inactive" or was unlabeled based upon accelerometer data. Data from "active" blocks are plotted in red and "inactive" blocks are plotted in blue. For the neuron 1 data set (presented in Fig. 1a,c–e) there are 438 data blocks. Blocks in which the maximum accelerometer magnitude (MAM) was greater than 1.25 g were labeled "active" (40% of 438 blocks) and blocks in which the MAM was less than 1.15 g were labeled "inactive" (52% of 438 blocks). These thresholds were selected to roughly balance the number of "active" and "inactive" blocks with the ratio of day (lights on) versus night (lights off) blocks (as we expect low activity when the lights are off), while retaining a 0.1 g margin between classifications.

Figure 1d,g was generated by down sampling the accelerometer data to 100 Samples/s. Firing rates in Fig. 1c,f were calculated with a 1 second interval (a hamming window was used as a lowpass filter). LFP power in Fig. 1e,h was estimated across the 5 minute blocks by integrating power over the 5–25 Hz frequency band. As described in Section III-A, this band was well differentiated between "active" and "inactive" periods.

From the accelerometer data (Fig. 1d,g), it is clear that the monkey was more physically active during the day, and as expected, firing rates tend to be higher during these periods. Notice that LFP power was generally lower during these periods. During the battery swap periods (pink bands) the monkey was head posted and so the accelerometer magnitude remained flat at 1 g. During these periods, few movements

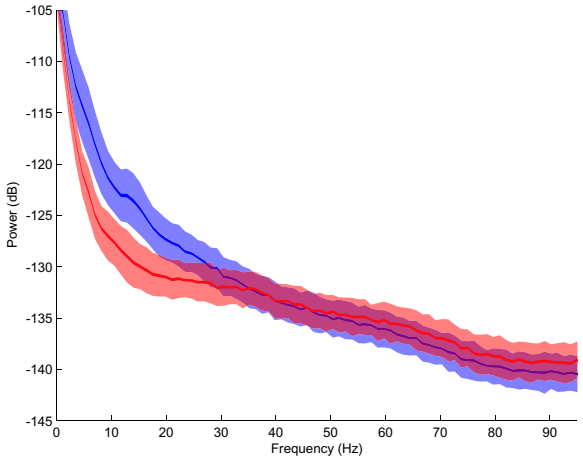

Fig. 2. Power spectral density (PSD) recorded during "active" (red) and "inactive" (blue) periods. The thin lines are the mean PSDs and the standard error of the mean is represented by their thickness. The thickness of the wider translucent lines are the standard deviations. Each PSD is calculated over 5 minutes of data and their distributions were taken from data across the 54 hour data set for neuron 1. (`D20060302.ch2u1`)

are made and consequently firing rates are reduced. These trends were consistent across two data sets collected from different electrodes and at different times. LFPs recorded simultaneously from a second channel show similar patterns.

A. Local Field Potential

As shown in figure 2, the mean LFP power differed between "active" and "inactive" periods in the 2–30 Hz and 50–100 Hz frequency bands. For the majority of this range the standard deviations are large relative to the difference in the mean; this relationship makes power changes in these bands an unreliable classifier for activity level. The 5–25 Hz band was well separated, so the power in this range should be used to develop a reliable classifier. This differentiation in LFP power

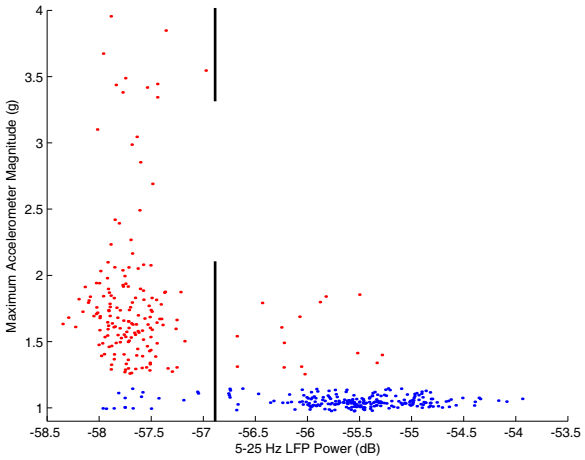

Fig. 3. 5–25 Hz LFP power versus maximum accelerometer event in a 5 minute block. Data points are from "active" (red) and "inactive" (blue) blocks across the 54 hours data set for neuron 1's channel. (`D20060302.ch2`)

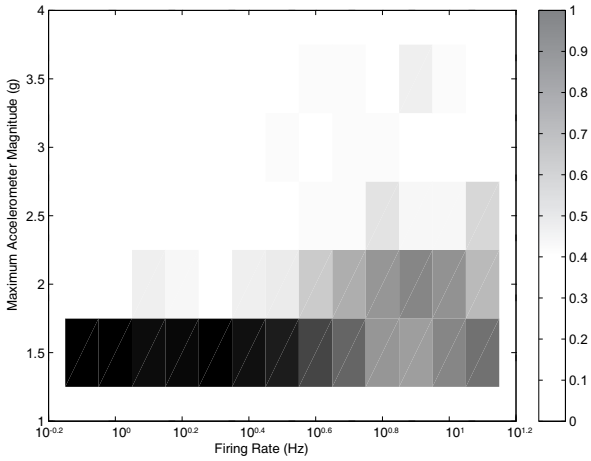

Fig. 4. Probability of maximum accelerometer event for a given firing rate. Note that firing rate is plotted on the log scale. Firing rate was calculated over a 5 minute window for data across the 54 hour data set of neuron 1. (`D20060302.ch2u1`)

is consistent with results in [9] showing that 10–100 Hz LFP activity diminished during movement.

Figure 3 plots 5–25 Hz LFP power versus MAM for each 5 minute block. In general, "active" (red) and "inactive" (blue) blocks are well separated by thresholding LFP power (as shown by the vertical dashed line). When we classified the activity level of blocks by thresholding LFP power at -57.25 dB, 91% of "active" blocks and 94% of "inactive" blocks were correctly classified. Results were similar for a second channel: 90% of "active" blocks and 89% of "inactive" blocks correctly classified with a threshold of -132.5 dB. Note that these results were obtained by manually setting a threshold upon visual examination of Fig. 3 and the corresponding plot for neuron 2; further work is necessary to assess the effectiveness of automated learning techniques. Head posting during "pit stops" may have resulted in lower estimates of performance, as the accelerometer was held in a fixed position even if the monkey was active during these periods.

B. Firing Rate

Figure 4 shows the probability distribution of the MAM for a 5 minute block as a function of firing rate over this period. The mean and variance of the MAM increased as the firing rate increased; notice that the probability of small MAM remained high. The electrode was implanted in a region of PMd believed to be involved in motor planning and execution of arm movements [5]. If arm movement are made while the head position remains fixed, firing rates could increase without large acceleration events. Also, motor plans can be generated and subsequently canceled. Thus, absolute firing rate may not be the best proxy for activity level.

Figure 5 shows the autocorrelation of firing rate for neuron 1 during "active" and "inactive" blocks. The firing rate was integrated over 100 ms windows and autocorrelations were calculated for each 5 minute block; the resulting distributions were plotted. The decay rate of the autocorrelation function is slower for "active" periods than "inactive" periods.

Higher firing during "active" periods (as shown in figures 1 and 4) does not explain this change in decay rate. If the firing rate was well modeled by a homogeneous Poisson distribution for each block, then firing rates between neighboring counts in a block would be independent and the autocorrelation function would be a delta function. This feature of the firing rate distributions was confirmed by randomly permuting the count for each 100 ms time bin to retain the firing rate distribution while eliminating temporal patterning; as expected, the resulting autocorrelations for both activity levels approach the delta function. Also, If firing rate encodes arm movements in a smooth and continuous manner, we expect real movements to result in smoother transitions in firing rate (and a slower decay rate in the autocorrelation function).

Also note the slight peaks around 1.5 and 3 seconds in the autocorrelation for "active" blocks. Through visual observation of behavior and accelerometer channel analysis, these peaks are consistent with an occasional, natural, and repetitive full body motion that occurred at a frequency of $\sim$0.75 Hz. During this activity both arms moved in synchrony from side to side. Since the behavior is well stereotyped, it may induce oscillatory firing at the movement frequency.

C. Circadian Rhythms

Given that "active" and "inactive" periods tended to occur during day and night, respectively, the variations in firing rate and LFP might be explained, in part, by circadian rhythms (or direct modulation by light level). Perhaps 5–25 Hz LFP power are increased and firing rates are depressed by an internal clock. However, for blocks with a single activity condition (either "active" or "inactive"), the differences between day and night for both LFP and firing rate were at least an order of magnitude smaller than the difference between "active" and "inactive" blocks during either time period. This suggests that circadian rhythms do not heavily influence these effects.

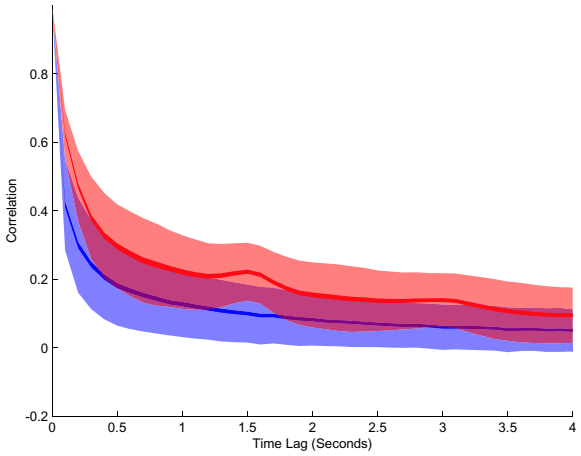

Fig. 5. Autocorrelation of neuron 1 firing rates for "active" (red) and "inactive" (blue) blocks. Firing rate integration time was 100 ms. The thin lines are the mean correlations and their thickness represents the standard error of the mean. The thickness of the wider translucent lines is the standard deviation. (`D20060302.ch2u1`)

IV. Discussion

Practical neural prosthetic systems should work well under varied conditions. We can begin to understand these conditions as contexts, defined here as a set of behavioral states and/or goals (such as active vs. inactive or discrete target selection vs. continuous pursuit). A switch in context may change the dynamics of observed neural signals; a neural prosthetic must be sensitive to these changes. In this paper, we examine a very simple pair of contexts — physically active and inactive. The monkey moved freely, so we could register these periods with an accelerometer. For an immobile patient, however, we must determine the *intent* to be physically active or inactive.

As shown in Figs. 2 and 3, LFP is a promising proxy for activity level. Firing rate can also be used for this purpose, as its autocorrelation is dependent on activity level (Fig. 5). However, LFP power measurement consumes less battery power than firing rate measurement (a low-power LFP power measurement circuit is described in [10]), potentially enabling a power efficient implant "sleep" mode when the user is inactive. When LFP power falls below a defined threshold, indicating that the user is active, the prosthetic can switch out of this "sleep" mode.

In future studies we plan to examine subtler context changes. Some contexts may require less data for acceptable performance; under these conditions we can conserve power by disabling a subset of the neural channels. Under different contexts, users may require different sets of behavioral responses (such as discrete target selection vs. continuous motion) or the underlying dynamics of the observed cortical area may change drastically; we would like to respond to these concerns by switching the decoding model according to context. By identifying contexts and adjusting hardware configuration accordingly, it may be possible to boost performance in terms of power consumption and decoding accuracy.

The presence of an identifiable repetitive natural behavior (as discussed in Section III-B), demonstrates the ability to identify behavior from primate neural recordings across multiple days. Such an ability coupled with advanced behavioral monitoring (such as chronically implanted EMG electrodes or motion tracking), can enable the exploration of questions that have been unapproachable until now. Mining large data sets of free behavior to find neural correlates may help us to develop new controlled experiments; such data sets are also necessary for testing and developing neural prosthetics systems with the ability to operate autonomously over extended periods of time.

V. Conclusion

In this paper we begin to analyze the first set of multiday neural and accelerometer data from area PMd in a freely behaving primate using the HermesB system. These data show that for time lags on the order of seconds the autocorrelation of firing rate is higher during physically active periods than during inactive periods; this suggests greater temporal correlation in firing rate during physical activity. An analysis of the power spectrum of broadband neural data demonstrates that 5–25Hz LFP power decreases during periods of physical activity, which can be used to turn implant processing on and off with little power consumption.

Acknowledgment

The authors would like to thank Dr. Mark Churchland and Byron Yu for enlightening conversations and advice and Mackenzie Risch for expert veterinary care.

References

[1] M. D. Linderman, V. Gilja, G. Santhanam, A. Afshar, S. Ryu, T. H. Meng, and K. V. Shenoy, "An autonomous, broadband, multi-channel neural recording system for freely behaving primates," in *Proc. of Conf. of IEEE EMBS*, 2006, submitted.

[2] J. Mavoori, A. Jackson, C. Diorio, and E. Fetz, "An autonomous implantable computer for neural recording and stimulation in unrestrained primates," *J. Neurosci. Methods*, vol. 148, pp. 71–77, 2005.

[3] I. Obeid, M. A. L. Nicolelis, and P. D. Wolf, "A multichannel telemetry system for single unit neural recordings," *J. Neurosci. Methods*, vol. 133, pp. 33–38, 2004.

[4] M. D. Linderman, V. Gilja, G. Santhanam, A. Afshar, S. Ryu, T. H. Meng, and K. V. Shenoy, "Neural recording stability of chronic electrode arrays in freely behaving primates," in *Proc. of Conf. of IEEE EMBS*, 2006, submitted.

[5] M. Churchland, B. M. Yu, S. I. Ryu, G. Santhanam, and K. V. Shenoy, "Neural variability in premotor cortex provides a signature of motor preparation," *J. Neurosci.*, vol. 26, pp. 3697–3712, 2006.

[6] N. Hatsopoulos, J. Joshi, and J. G. O'Leary, "Decoding continous and discrete behaviors using motor and premotor cortical ensembles," *J. Neurophysiol.*, vol. 92, pp. 1165–1174, 2004.

[7] M. Sahani, "Latent variable models for neural data analysis," Ph.D. dissertation, California Institute of Technology, 1999.

[8] Z. S. Zumsteg, C. Kemere, S. O'Driscoll, G. Santhanam, R. E. Ahmed, K. V. Shenoy, and T. H. Meng, "Power feasbility of implanatable digital spike sorting circuits for neural prosthetic systems," *IEEE Trans. Neural Syst. Rehab. Eng.*, vol. 13, pp. 272–279, 2005.

[9] J. Donoghue, J. Sanes, N. Hatsopoulos, and G. Gyngyi, "Neural discharge and local field potential oscillations in primate motor cortex during voluntary movements," *J. Neurophysiol.*, vol. 79, pp. 159–173, 1998.

[10] R. Harrison, G. Santhanam, and K. Shenoy, "local field potential with low-power analog integrated circuits," in *Proc. of EMBS*, 2004, pp. 4067–4070.